13th World Conference on Earthquake Engineering
Vancouver, B.C., Canada
August 1-6, 2004
Paper No. 2357

NEW METHOD FOR ESTIMATING SEISMIC RESPONSE OF FRAME STRUCTURES CONSIDERING COLLAPSE MECHANISM

Yo HIBINO[1], Hisashi UMEMURA[2] and Toshikatsu ICHINOSE[3]

SUMMARY

For seismic performance-based design, it is important to evaluate structural performance for various seismic excitations. The absorbed energy in a structure, which is closely related to the seismic damages, can be an index to evaluate a building by performance. The energy attributed to the total and collapse mechanisms were evaluated for RC and steel frame structures under 84 ground motions and were compared each other to study energy demand on structure. The maximum drifts gained by dynamic response analyses were compared with the cumulative plastic story drifts evaluated from energy. Then, a factor which indicates the relationships between cumulative plastic story drifts and dynamic responses were obtained. The estimation method was presented using the factor and its applicability was evaluated.

INTRODUCTION

Recently, the main stream of seismic design tends to evaluate a building by performance and it is known as performance-based seismic design. If the maximum response deformation for a building can be estimated, a designer can tell the owner of the building the seismic performance exactly and the destructive seismic damage will be prevented. Chopra [1] presented Modal pushover analysis (MPA) procedure to evaluate the story drift. Chintanapakdee [2] evaluated the MPA procedure for generic frames and showed the availability of the method. The MPA procedure is suitable to evaluate the maximum story drifts considering the effects of collapse modes by using only a pushover analysis without doing the dynamic response analysis. However, the MPA procedure has not been successfully applied to buildings with weak or soft story.

Akiyama [3] expressed that the absorbed energy in a structure can be an index to evaluate the seismic performance of buildings by using a multi-degree-of-freedom (MDOF) system. Chung-Che [4] presented a procedure that can predict the damage distribution of low- to medium-rise frames from the absorbed energy by converting MDOF frame into an equivalent single-degree-of-freedom system for each of the first and two modes.

[1] Graduate Student, M. Eng., Nagoya Inst. of Tech., Nagoya, Japan. Email: hibino@manage.nitech.ac.jp
[2] Assist. Prof., Dr. Eng., Nagoya Inst. of Tech., Nagoya, Japan. Email: h.umemura@nitech.ac.jp
[3] Prof., Dr. Eng., Nagoya Inst. of Tech., Nagoya, Japan. Email: ich@nitech.ac.jp

In this paper, seismic story drifts were estimated by energy demand theory considering the collapse mode of RC and steel frame structures. The estimation procedure was valid for buildings with either total or story mechanisms.

STRUCTURAL MODELS SYSTEMS, GROUND MOTIONS

Configuration and Strength for RC

The structural systems were frame structures with 9 stories and 6 m spans. Equal story heights of 3.5 m and story weights of 768 kN were assumed for the structures. Figure 1 shows the elevation and member sizes of columns and beams for RC structures.

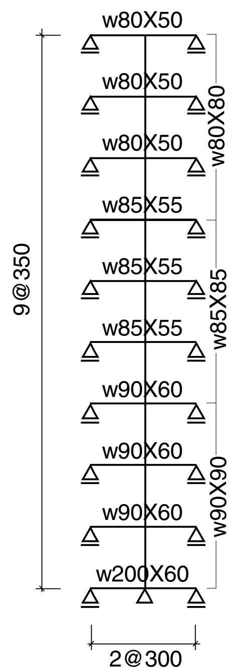

Figure 1. Elevation and member sizes (Unit = cm)

The RC hysteretic model was trilinear as shown in Figure 2. Beams and columns of RC were modeled as members with inelastic flexural springs at both the ends. At these springs, the Takeda model [5] was used to represent the flexural deformation. The Young's modulus was assumed as 2.1×10^4 N/mm^2. The elastic stiffness of members was calculated from their overall dimensions. The cracking flexural strengths of members were assumed as one-third of the corresponding yield strengths. The post-yield stiffness was assumed as 0.001 times the elastic stiffness and the post-yield stiffness-reducing ratio was assumed as 0.3.

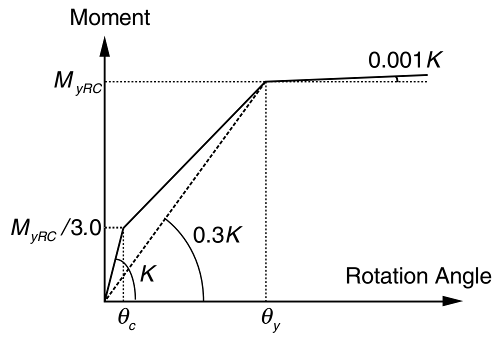

Figure 2. Hysteretic model of RC members

The yield strengths of members, M_{yRC}, were assigned in accordance with the bending moments that were obtained in elastic analysis using the Japanese A_i lateral seismic force distribution for the base shear coefficient of 0.3. The center column of table 1 shows the results of the elastic analysis. The yield strengths of the beams were set to be the bending moment of the elastic analysis as shown in the right column of table 1 except for the roof and the foundation beam where the moments were multiplied 1.5 and 3, respectively. The yield strengths of columns were set to be the averages of the bending moments of at the top and at the bottom of the columns. The beam stiffness was doubled to account for the effects of adjacent floor slabs. The damping factor was 0.05 in proportion to the tangential stiffness.

Table 1. Result of elastic analysis and yield strength (Unit = kN·m)

	Result of elastic analysis			Yield strength	
Story	Column top	Column base	Beam	Column	Beam
9	1129	649	565	912	1752
8	1641	1309	1168	1475	1168
:	:	:	1628	:	1628
2	3396	3538	:	3467	:
1	2661	4594	3099	3628	3099
Foundation			2297		9297

Configuration and Strength for Steel

The structural systems for steel were a frame with 9 stories and 6 m spans. The story heights were 3.5 m and the equal story weights were 768 kN which is as the same as the RC model. The hysteretic model of steel was elastic-plastic bilinear model as shown in Figure 3. The Young's modulus was assumed as 2.1×10^5 N/mm^2. The yield strengths of members were the same as the RC model. The moments of inertia of members, I, were determined by $I = (I_S / M_{yS}) \times M_{yRC}$, where M_{yRC} is the yield strength of the RC model and I_S and M_{yS} are, respectively, the moment of inertia and the yield strength of each sections given in one of the design examples in the Design Standard for Steel Structures (Architectural Institute of Japan [6]). The beam stiffness was doubled to account for the effects of adjacent floor slabs. The post-yield stiffness was assumed as 0.01 times the elastic stiffness and the damping factor was 0.05 in proportion to the tangential stiffness.

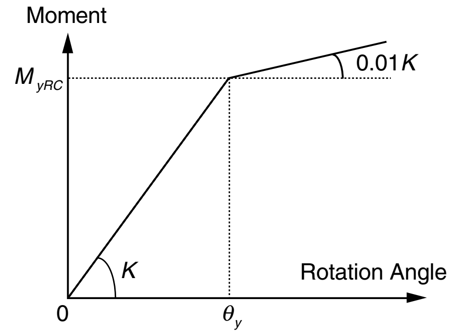

Figure 3. Hysteretic model of steel members

Analytical Models

The analytical models were based on the prototype structure by multiplying the flexural strengths of the columns by a strength factor, ψ_i, from a range of 0.7, 0.8 … to 1.3. Two types of models for each structure, characterized by the strength factor distribution, were used: a "uniform model" where the strength factor was distributed equally and a "weak model" where the strength factor was lower in the middle story. The flexural strengths of all the columns for the weak model were multiplied by the strength factor of 0.8, 0.9 … or 1.2 except for the weak story whose strength factor was fixed to 0.7 (see Figure 4).

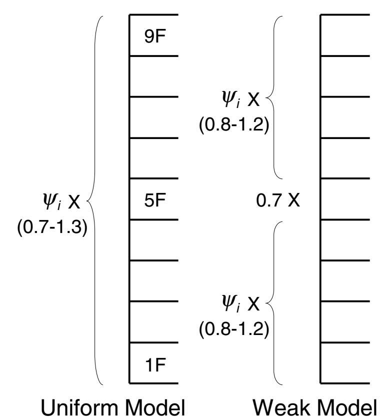

Figure 4. Application of strength factor

Input Ground Motions

The input ground motions used were four recorded earthquake ground motions: "El Centro" at Imperial Valley, "Hachinohe" at Tokachi-oki, "KJMA" at Kobe and "Sylmar" at Northridge (see Table 2). In addition, twenty-earthquake grounds motions were generated by the wavelet transform (Umemura [7]) from each original ground motion. The spectra of generated ground motions are similar to the originals but the phase characters are different. Among them, input factor, 2.46 and 2.62, were multiplied to the El Centro and the Hachinohe records, respectively, to make its value of peak velocity equal 100 cm/sec

Table 2. Input ground motions

Earthquake	Station	PGA (cm/sec^2)	Factor
Imperial Valley, 1940	El Centro NS	321.92	2.46
Tokachi-oki, 1968	Hachinohe NS	216.81	2.62
Northridge, 1994	Sylmar NS	936.47	1
Kobe, 1995	KJMA NS	825.76	1

Figure 5 shows the elastic response spectra of original and generated El Centro ground motions with damping ratio of 5%. The thick line represents the spectra of original ground motion.

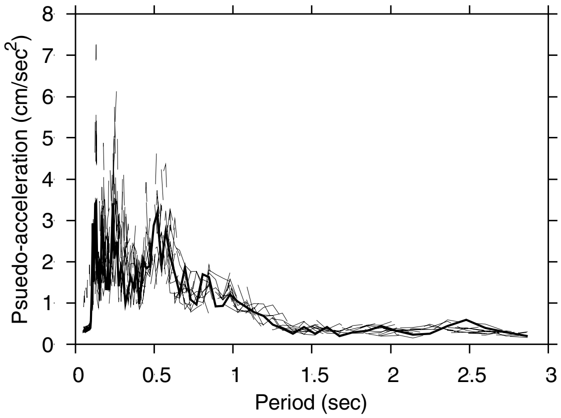

Figure 5. Pseudo-acceleration spectra of original and generated El Centro ground motions. Damping ratio = 5%

DEFINITION OF ENERGY AND STORY DRIFTS

Cumulative Plastic Energy

The cumulative plastic energy, W_{psi}, which is due to the *i*th story mechanism, is defined as the hysteretic energy consumed at the plastic hinges defined by Equation 1 and shown in Figure 6a. The cumulative plastic energy at the first and roof story are doubled for the energy consumed at top and bottom of columns, respectively. The cumulative plastic energy, W_{pt}, which is due to the total mechanism, is the total of hysteretic energy at the plastic hinges in Figure 6b and defined by Equation 2. Where, the cumulative plastic energy of the first and roof story are subtracted to prevent a double count of energy of the first and *n*th story collapse.

$$\begin{cases} W_{psi} = \sum {}_c W_{psi} & \text{for } i \neq 1, n \\ W_{ps1} = 2 {}_c W_{ps1} & \text{for } i = 1 \\ W_{psn} = 2 {}_c W_{psn} & \text{for } i = n \end{cases} \tag{1}$$

$$W_{pt} = {}_c W_{pt1} + {}_c W_{ptn} + \sum_{i=2}^{n} {}_b W_{pti} - \left({}_c W_{ps1} + {}_c W_{psn} \right) \tag{2}$$

where *n* is the number of stories.

Figure 6. Plastic hinges

Note that the energy defined above includes the energy before the yielding (but after cracking).

Cumulative Plastic Story Drift

The cumulative plastic story drift, R_{psi}, which is due to the ith story yield mechanism, is shown in Figure 7a and defined by Equation 3, because $R_{psi}\cdot h_i$ represents the story displacement.

$$R_{psi} = \frac{W_{psi}}{Q_{si} h_i} \tag{3}$$

The cumulative plastic story drift, R_{pt}, which is due to the total mechanism, is shown in Figure 7b and defined by Equation 4, because $R_{pt}\cdot h_i$ represents the ith story displacement due to the total mechanism.

$$R_{pt} = \frac{W_{pt}}{\sum_{i=1}^{n} Q_{ui} h_i} \tag{4}$$

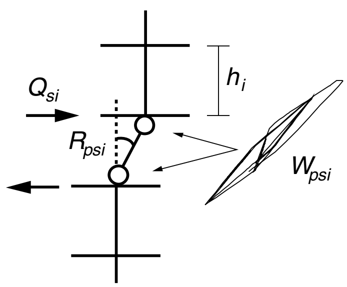

(a) Diagram of R_{psi}

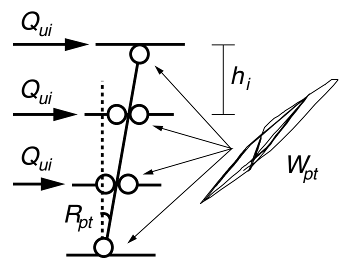

(b) Diagram of R_{pt}

Figure 7. Diagrams of R_{psi} and R_{pt}

Q_{ui} is the story shear force at a "Mechanism Point" obtained from the pushover analysis. The mechanism point is defined as shown in Figure 8, where the vertical axis is the base shear, Q_1, and the horizontal axis is the drift ratio which is the roof displacement, D_{top}, divided by the building height, H. The solid line represents the force-deformation curve. Q_u is the intersection of the vertical axis and the line connecting the analytical points where D_{top} / H are 0.02 and 0.015. The mechanism point is defined when the base shear force reaches Q_u. Q_{ui} and R_{ui} are the ith story drift and story shear at the mechanism point, respectively.

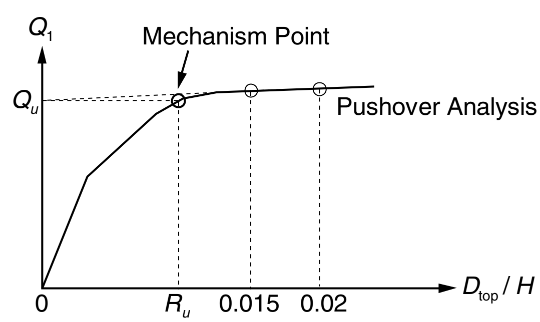

Figure 8. Mechanism point

PUSHOVER ANALYSIS RESULTS

Figure 9 shows the results of the pushover analysis. The axes are the relative story displacement and the story shear. The open circles represent the mechanism points on each story. In case of the uniform model of ψ_i=0.8, the column top and bottom of every story yielded. In case of the uniform model of ψ_i=1.2, the beams of all the stories except for the first and roof story yielded, so the total mechanism occurred. For the weak models with all strength factors, the story collapse occurred in the weak story.

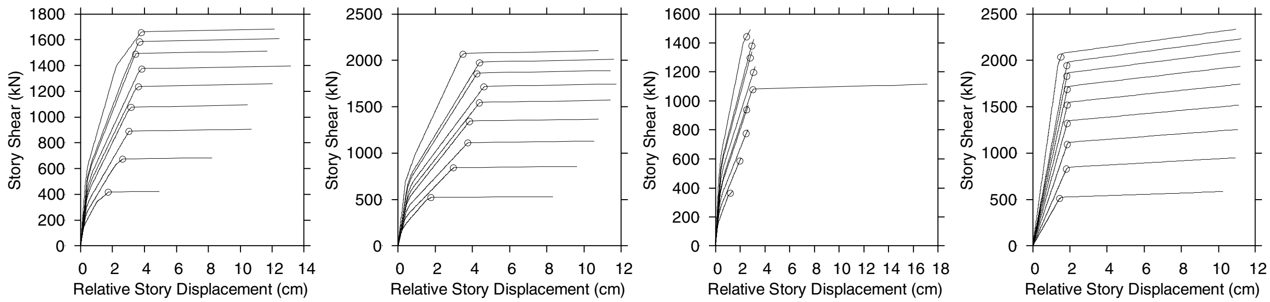

(a) RC (Uniform, ψ_i=0.8) (b) RC (Uniform, ψ_i=1.2) (c) RC (Weak, ψ_i=0.8) (d) Steel (Uniform, ψ_i=1.2)

Figure 9. Pushover analysis result

DYNAMIC RESPONSE ANALYSIS RESULTS

Relative Story Displacement

Relative story displacement for each model is shown in Figure 10. The vertical axis is the story number. The solid thin lines are the dynamic responses, the dashed line is the mean, and the chained line is the story displacement at the mechanism point.

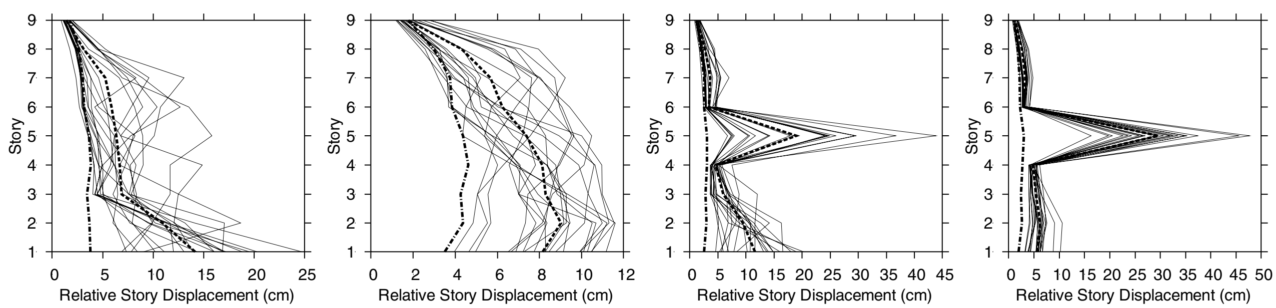

(a) RC (Uniform, ψ_i=0.8) (b) RC (Uniform, ψ_i=1.2) (c) RC (Weak, ψ_i=0.8) (d) RC (Weak, ψ_i=1.2)

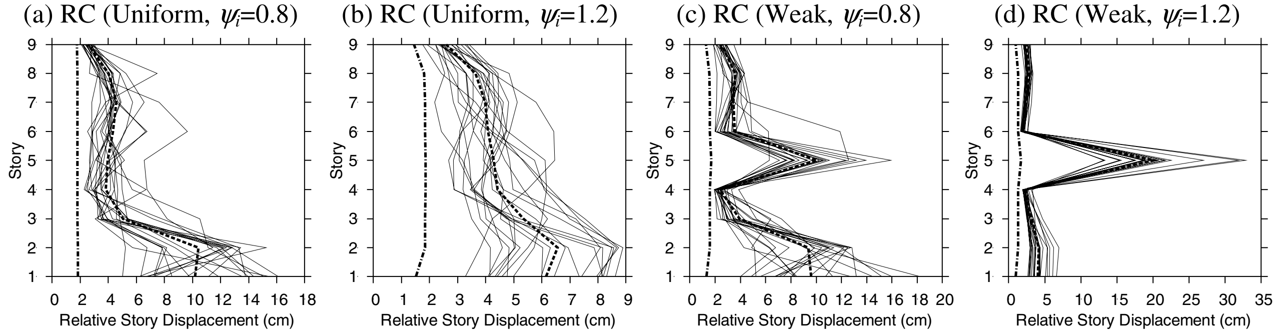

(e) Steel (Uniform, ψ_i=0.8) (f) Steel (Uniform, ψ_i=1.2) (g) Steel (Weak, ψ_i=0.8) (h) Steel (Weak, ψ_i=1.2)

Figure 10. Relative story displacement (Sylmar)

It is observed that the maximum story displacement of the RC model is larger than that of the steel model. For the uniform model, the damages in case of ψ_i=0.8 concentrated more than that of ψ_i=1.2. However, in case of ψ_i=1.2, some concentration were observed in each dynamic response of upper (7 and 8) and lower (1 and 2) stores due to higher mode effects. For the weak model of ψ_i=0.8, the damages concentrated in 1st and 2nd stories as well as in the weak 5th story, particularly for the steel model.

Comparison of Cumulative Plastic Energy

Figure 11 shows the relationships between the cumulative plastic energy and the strength factor for each model. The triangle and square symbols represent the cumulative plastic energy ΣW_{psi} and W_{pt}, respectively; also, ΣW_{psi} is the total of W_{psi} in each frame. The dashed and chained line are the averages of cumulative plastic energy obtained from dynamic response analyses under the 21 ground motions and the solid line is the total of average of ΣW_{psi} and W_{pt}.

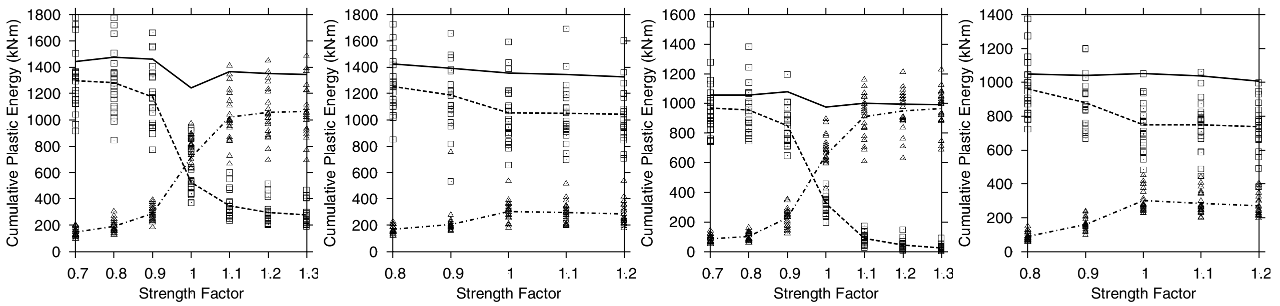

(a) RC (Uniform) (b) RC (Weak) (c) Steel (Uniform) (b) Steel (Weak)

Figure 11. Relationships between cumulative plastic energy and strength factor (Sylmar)

It is observed that ΣW_{psi} and W_{pt} varied with the strength factor. However, the total of energy is almost constant irrespective of with or without weak story for each model. That is, the cumulative plastic energy is independent of the strength distribution. While, ΣW_{psi} is nearly zero when the strength factor is 1.3, that tendency is not observed for the RC model. The reason is attributable to the energy absorbed before yielding but after cracking, which does not exist for the steel model.

Definition of Plastic Component of Drift

The elastic component of the drift, R_{ei}, which is shown in Figure 12 is defined by Equation 5, so that the area, S_i, which is enclosed by the pushover curve till the mechanism point is the same as the area which enclosed by the equivalent bilinear curve.

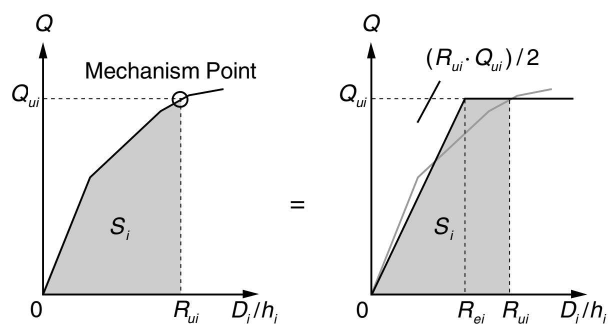

Figure 12. Replacement pushover curve with equivalent bilinear curve

$$R_{ei} = 2 \times \left(R_{ui} - \frac{S_i}{Q_{ui}} \right) \tag{5}$$

where D_i is the ith story displacement and h_i is the story height.

The plastic component of the maximum drift, ${}_dR_{pi}$, is defined by Equation 6, where ${}_dR_{\max i}$ is the maximum drift given by the dynamic response analysis.

$$ {}_{d}R_{pi} = {}_{d}R_{\max i} - R_{ei} \tag{6} $$

Comparison between Cumulative Plastic Story Drifts and Maximum Drift

Figure 13 shows the relationships between the cumulative plastic story drifts and the plastic component of the maximum drifts. Each plot in Figure 13a and c shows the data of each story, whereas that in Figure 13b and d shows the data of average. The cumulative plastic story drift, R_{psi} was multiplied by the ratio of the cumulative plastic energy to total energy, W_{total}, because there was considerable amount of W_{pt} even for the case of ψ_i=0.7. The cumulative plastic story drift, R_{pt}, was similarly multiplied by W_{total} / W_{pt}. The solid line is the regression line, which was obtained by the method of least squares, and the slope is indicated at the upper left on the graph with the equation $f(x)$ and correlation coefficient r is indicated, too.

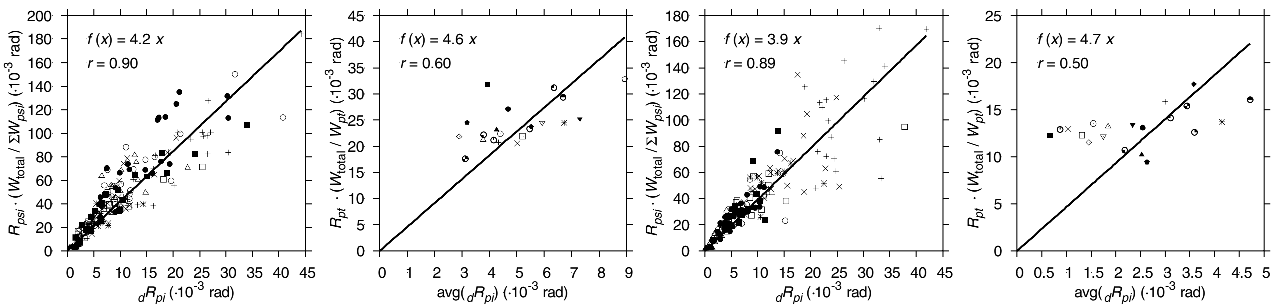

(a) $R_{psi} - {}_{d}R_{pi}$ (El Centro, ψ_i=0.7)

(b) $R_{pt} - \text{avg}({}_{d}R_{pi})$ (El Centro, ψ_i=1.3)

(c) $R_{psi} - {}_{d}R_{pi}$ (Hachinohe, ψ_i=0.7)

(d) $R_{pt} - \text{avg}({}_{d}R_{pi})$ (Hachinohe, ψ_i=1.3)

Figure 13. Relationships between cumulative plastic story drifts and plastic component of maximum drifts (RC, Uniform)

It is observed that R_{psi} are closely related with ${}_{d}R_{pi}$ for both ground motions. Also, the plots of R_{pt} and avg(${}_{d}R_{pi}$) are closely related, too.

Correlation Coefficient

The correlation coefficient r of each model is shown in Figure 14. The solid line is the correlation coefficient of R_{psi} and the chained line is that of the R_{pt}.

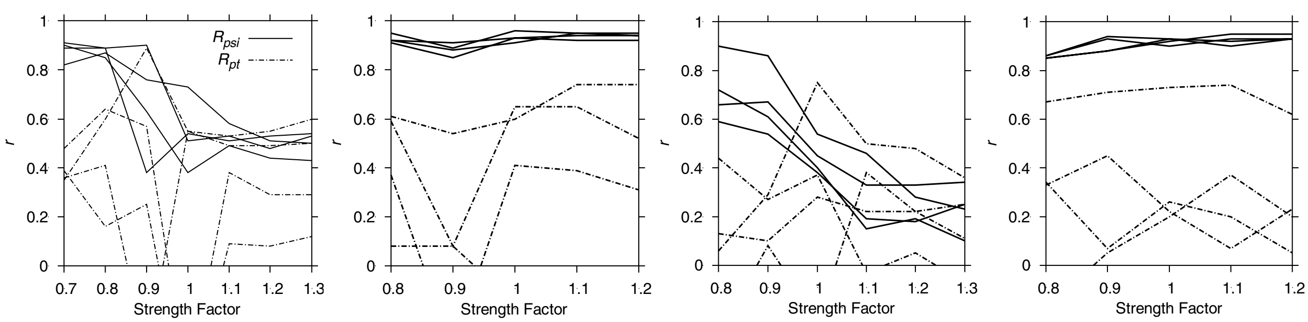

(a) RC (Uniform)

(b) RC (Weak)

(c) Steel (Uniform)

(d) Steel (Weak)

Figure 14. Correlation coefficient of each model and strength factor

It is observed that for the uniform model, the correlation coefficient of R_{psi} is nearly one in case of the strength factor is less than 0.9, whereas the correlation coefficient of R_{psi} is similar to that of R_{pt} in case of the strength factor is larger than 1.1 (see Figure 14a and c). For the weak model, the correlation coefficient of R_{psi} is nearly one in all cases, whereas the correlation coefficient of R_{pt} is lower than that of R_{psi} in all cases (see Figure 14b and d). Note that R_{psi} and R_{pt} are, respectively, dominant in case that the story and total mechanisms occur. Therefore, for the uniform model, R_{psi} is available in case of the strength factor is less than 0.9 and R_{pt} is available in case of the strength factor is larger than 1.1. The reason why the correlation coefficient of R_{psi} is larger than that of R_{pt} and constant in all cases for the weak model is attributable to the collapse mechanism; therefore, R_{pt} is meaningless for evaluating the dynamics responses.

Slope of Regression Line

The slopes of the regression line are shown in Table 3, where n_{Rpsi} and n_{Rpt} are the slopes of the regression lines, respectively, between R_{psi} and ${}_dR_{pi}$, and between R_{pt} and avg(${}_dR_{pi}$). Also, the slopes are shown in cases that the correlation coefficient is high. The fist line shows the strength factor.

Table 3. Slope of regression line

		Weak					Uniform					
		0.8	0.9	1.0	1.1	1.2	0.7	0.8	0.9	1.1	1.2	1.3
		RC										
El Centro	n_{Rpsi}	4.4	3.8	4.8	4.8	4.7	4.2	4.6	3.9	–	–	–
	n_{Rpt}	–	–	–	–	–	–	–	–	4.8	4.6	4.6
Hachinohe	n_{Rpsi}	3.9	3.9	4.1	4.1	3.9	3.9	3.9	3.9			
	n_{Rpt}	–	–	–	–	–	–	–	–	5.1	4.8	4.7
Sylmar	n_{Rpsi}	2.7	2.5	3.2	3.1	3.3	2.7	2.6	2.5	–	–	–
	n_{Rpt}	–	–	–	–	–	–	–	–	2.8	2.7	2.7
KJMA	n_{Rpsi}	3.3	3.2	3.4	3.4	3.6	3.6	3.5	3.3	–	–	–
	n_{Rpt}	–	–	–	–	–	–	–	–	2.8	2.8	2.8
		Steel										
El Centro	n_{Rpsi}	4.1	4.9	5.8	5.9	6.1	3.1	3.1	3.1	–	–	–
	n_{Rpt}	–	–	–	–	–	–	–	–	3.1	3.3	3.7
Hachinohe	n_{Rpsi}	3.5	4.2	4.5	4.7	4.5	2.4	2.4	2.6	–	–	–
	n_{Rpt}	–	–	–	–	–	–	–	–	2.5	3.0	3.4
Sylmar	n_{Rpsi}	2.7	3.4	4.4	4.2	4.3	2.4	2.4	2.3	–	–	–
	n_{Rpt}	–	–	–	–	–	–	–	–	2.5	2.7	2.7
KJMA	n_{Rpsi}	3.6	4.4	5.2	5.8	6.0	3.1	3.0	2.9	–	–	–
	n_{Rpt}	–	–	–	–	–	–	–	–	3.0	3.4	3.8

It is observed that the slopes, n_{Rpsi}, are almost the same in cases of the same ground motions for the RC model. n_{Rpt} has a similar tendency. However, n_{Rpt} is larger than n_{Rpsi} in most cases for the uniform model. For the steel weak model, n_{Rpsi} increases as the strength factor increases in any cases.

ESTIMATION OF STORY DRIFTS

By using the slopes, the plastic component of estimated story drift is defined by Equation 7. And the estimated story drift, $R_{\max i}$, is defined by Equation 8.

$$R_{pi} = \frac{R_{psi}}{n_{Rpsi}} + \frac{R_{pt}}{n_{Rpt}} \tag{7}$$

$$R_{\max i} = R_{pi} + R_{ei} \tag{8}$$

Figure 15 shows the relationships between the plastic component of estimated story drift, R_{pi}, and the plastic component of maximum drift, ${}_dR_{pi}$, when the slopes, n_{Rpsi} and n_{Rpt} are used in case of ψ_i=0.7 and ψ_i=1.3, respectively, because in each case, the collapse mechanism is clear and availability of those slopes are reliable. The regression line is displayed in the upper left on graph and the correlation coefficient *r* is displayed, too. Each graph contains the models in cases of all strength factors, then the plots of data are about 1323 and 945, respectively, for the uniform and weak models.

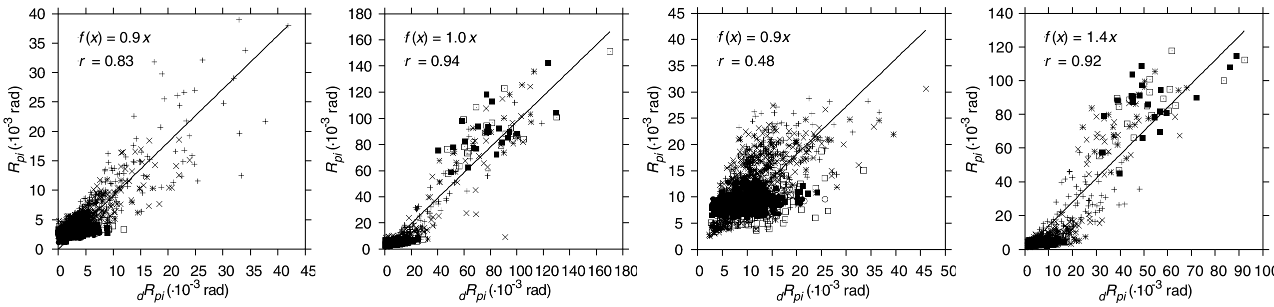

(a) RC (Uniform, Hachinohe) (b) RC (Weak, Sylmar) (c) Steel (Uniform, KJMA) (d) Steel (Weak, Sylmar)

Figure 15. Relationships between plastic components of estimated story drifts and plastic components of maximum drifts.

Although, there is dispersion between the estimated story drifts and dynamic responses, the correlation coefficient is nearly one for the RC model and the dynamic responses agreed with the estimated story drifts. For the steel uniform model, the dispersion is large in any cases and the correlation is small. The reason of that is attributable to the dispersion of the dynamic responses of the steel frame shown in Figure 10e and f. On the other hand, for the steel weak model, the correlation coefficient is high and the estimated story drifts agree with the dynamic responses in the weak story, except for the cases that the story drifts are small.

CONCLUSIONS

This paper presented an estimation method for evaluating the seismic story drifts using the hysteretic energy considering the collapse mechanisms. The method is summarized below:

1. Evaluate the hysteretic energy due to the total and story collapse mechanisms considering the column-to-beam strength ratio.
2. Estimate the cumulative plastic story drifts due to the two mechanisms using Equation 3 and 4.
3. Divide the values above by factors which depend on the characteristics of ground motion to obtain the plastic component of the maximum drift using Equation 7.
4. Add the elastic component to the values above using Equation 8.

The presented method was verified for the RC and steel models. The seismic story drifts were evaluated by the estimated story drifts, although there is some dispersion in case of small story displacement.

REFERENCES

1. Anil K. Chopra, Rakesh K. Goel "A modal pushover analysis procedure for estimating seismic demands for buildings" Earthquake Engineering & Structural Dynamics. Vol. 31, 2002: 561-582.
2. Chatpan Chintanapakdee, Anil K. Chopra "Evaluation of modal pushover analysis using generic frames" Earthquake Engineering & Structural Dynamics. Vol. 32, 2003: 417-442.
3. Akiyama H. "Earthquake-resistant Limit-state Design for Buildings" University of Tokyo Press: Japan. 1985.

4. Chung-Che Chou, Chia-Ming Uang "A procedure for evaluating seismic energy demand of framed structures" Earthquake Engineering & Structural Dynamics. Vol. 32, 2003: 229-244.
5. Takeda T., Sozen M.A. and Nielson N.N. "Reinforced concrete response to simulated earthquakes" Journal of Structural Engineering. ASCE, Vol. 96, No. 4, 1970: 2557-2573.
6. Architectural Institute of Japan "Design standard for steel structures" Architectural Institute of Japan. 1973.
7. Umemura H, Dinh V. Thuat, Ichinose T. "Estimate of Story Response Displacement for RC Buildings. Part 1 Generation of ground motions with identical spectral amplitude and shape envelope" Summaries of Technical Papers of Annual Meeting. Architectural Institute of Japan. Structures IV, 2001: 677-678.